Report

Current Biology

Direct Electrical Stimulation in the Human Brain Disrupts Melody Processing

Graphical Abstract

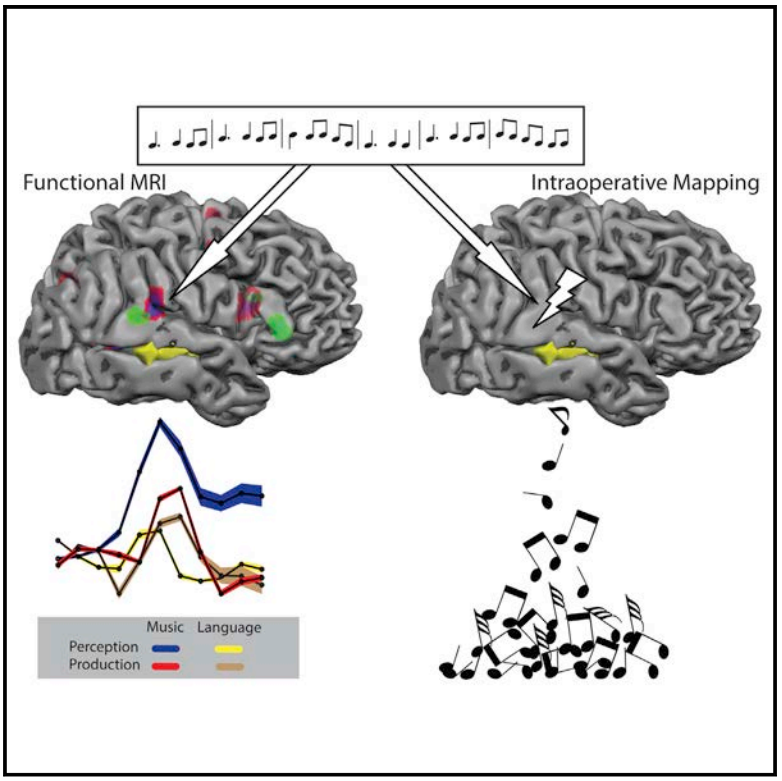

Authors

Frank E. Garcea, Benjamin L. Chernoff, Bram Diamond, ..., Elizabeth Marvin, Webster H. Pilcher, Bradford Z. Mahon

Correspondence

mahon@rcbi.rochester.edu

In Brief

Garcea et al. show that intraoperative electrical stimulation of fMRI-identified music regions in the right posterior superior temporal gyrus causes music arrest and errors in pitch, while sparing language function.

Highlights

- Causal evidence for a role of the right superior temporal gyrus in music repetition
- Functional organization of music processing revealed using electrical stimulation
- A new paradigm for mapping music in the human brain during awake brain surgery
- Intraoperative awake mapping of melody processing in the right temporal lobe

Garcea et al., 2017, Current Biology 27, 2684–2691
September 11, 2017
http://dx.doi.org/10.1016/j.cub.2017.07.051

CellPress

Current Biology
Report

Direct Electrical Stimulation in the Human Brain Disrupts Melody Processing

Frank E. Garcea,[1,2,3] Benjamin L. Chernoff,[1] Bram Diamond,[1] Wesley Lewis,[1] Maxwell H. Sims,[1] Samuel B. Tomlinson,[4] Alexander Teghipco,[1] Raouf Belkhir,[1] Sarah B. Gannon,[4] Steve Erickson,[4] Susan O. Smith,[4] Jonathan Stone,[4] Lynn Liu,[5] Trenton Tollefson,[5] John Langfitt,[5] Elizabeth Marvin,[1,6] Webster H. Pilcher,[4] and Bradford Z. Mahon[1,2,3,4,5,7,*]

[1]University of Rochester, Department of Brain & Cognitive Sciences, 358 Meliora Hall, Rochester, NY 14627, USA
[2]University of Rochester, Center for Language Sciences, 358 Meliora Hall, Rochester, NY 14627, USA
[3]University of Rochester, Center for Visual Science, 274 Meliora Hall, Rochester, NY 14627, USA
[4]University of Rochester Medical Center, Department of Neurosurgery, 601 Elmwood Avenue, Rochester, NY 14642, USA
[5]University of Rochester Medical Center, Department of Neurology, 601 Elmwood Avenue, Rochester, NY 14642, USA
[6]University of Rochester, Eastman School of Music, 26 Gibbs Street, Rochester, NY 14604, USA
[7]Lead Contact
*Correspondence: mahon@rcbi.rochester.edu
http://dx.doi.org/10.1016/j.cub.2017.07.051

SUMMARY

Prior research using functional magnetic resonance imaging (fMRI) [1–4] and behavioral studies of patients with acquired or congenital amusia [5–8] suggest that the right posterior superior temporal gyrus (STG) in the human brain is specialized for aspects of music processing (for review, see [9–12]). Intracranial electrical brain stimulation in awake neurosurgery patients is a powerful means to determine the computations supported by specific brain regions and networks [13–21] because it provides reversible causal evidence with high spatial resolution (for review, see [22, 23]). Prior intracranial stimulation or cortical cooling studies have investigated musical abilities related to reading music scores [13, 14] and singing familiar songs [24, 25]. However, individuals with amusia (congenitally, or from a brain injury) have difficulty humming melodies but can be spared for singing familiar songs with familiar lyrics [26]. Here we report a detailed study of a musician with a low-grade tumor in the right temporal lobe. Functional MRI was used pre-operatively to localize music processing to the right STG, and the patient subsequently underwent awake intraoperative mapping using direct electrical stimulation during a melody repetition task. Stimulation of the right STG induced "music arrest" and errors in pitch but did not affect language processing. These findings provide causal evidence for the functional segregation of music and language processing in the human brain and confirm a specific role of the right STG in melody processing.

RESULTS

Patient AE is a 26-year-old male saxophonist and wind instrument teacher who presented in 2015 with a brain tumor medial to the right posterior middle temporal gyrus and undercutting the superior temporal gyrus (Figure 1A, tumor in yellow fill). Over a period of 6 months, the patient underwent extensive pre-operative functional magnetic resonance imaging (fMRI) and behavioral testing to localize music, language, and high-level visual processing and to ascertain his levels of performance with judgments of musical pitch, rhythm, and contour. Patient AE had no discernible cognitive or sensorimotor impairments and was in the normal range across all pre-operative neuropsychological tests assessing language, semantic memory, visual and auditory processing, and praxis knowledge (Table S1). He exhibited typical neural organization of language, high-level visual processing, and praxis knowledge (see Figure S1A for fMRI contrast maps and STAR Methods for all details). In this report, we focus on the relation between pre-operative fMRI studies of music processing and the behavioral effects of direct electrical stimulation to the right temporal lobe during the awake portion of his surgery.

Pre-operative fMRI and Behavioral Testing

In a first fMRI experiment designed to map music processing, the patient listened to a brief (3 s) piano melody [1] or spoken sentence on each trial [27], internally "rehearsed" the stimulus, and then overtly produced the stimulus (humming in the case of melodies, speaking in the case of language; task modeled directly after Hickok and colleagues [1]). Replicating prior studies using this paradigm [1, 2], there was increased blood oxygen level dependent (BOLD) contrast for melody processing compared to sentence processing in the right superior temporal gyrus (Figure 1A). A closer look at the gyral anatomy in coronal images (Figure S2) indicated that the "peak" of this activity was at the posterior aspect of the Sylvian fissure, likely in the superior temporal gyrus, and potentially involving the parietal operculum (see also surface rendering in Figure 1A). Event-related responses in that region were differentially driven by perception and rehearsal as opposed to production of the melodies (Figure 1A). Two control groups were assessed with the same fMRI experiment: one group was comprised of age- and education-matched musicians (n = 4); a second control group consisted of neurosurgery patients scanned pre-operatively

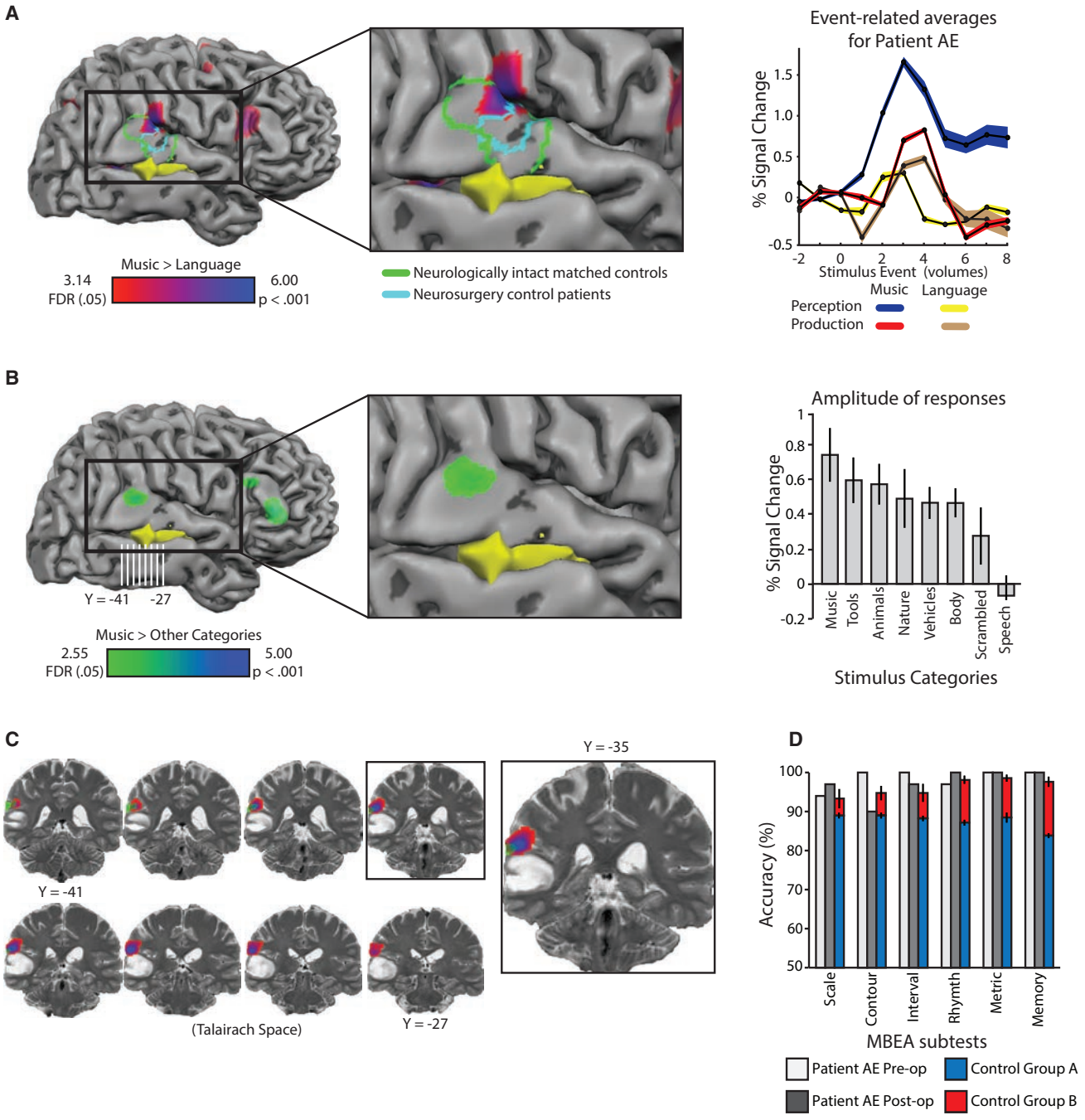

Figure 1. Music Processing in the Right Superior Temporal Gyrus

(A) Voxels exhibiting increased BOLD contrast for melody compared to sentence repetition in the vicinity of the right superior temporal gyrus (red-blue color scale; $t \geq 3.14$, whole-brain false discovery rate (FDR) $q < 0.05$; peak coordinate [57 −34 22]). The tumor is represented in yellow. A group of four neurologically intact age and music-education-matched control participants took part in the same experiment (data are plotted in green outline on patient AE's brain to facilitate comparison, $t \geq 2.51$, FDR $q < 0.05$). A separate group of ten neurosurgery patients also completed the same experiment pre-operatively (data plotted in cyan, $t \geq 2.26$, $p < 0.05$, uncorrected). Event-related time series indicate patient AE's neural responses in the right superior temporal gyrus were maximal for music perception. Error bars represent the standard error of the mean.

(B) There was increased BOLD contrast for music stimuli (e.g., guitar strumming, piano playing) compared to other categories of sounds (e.g., vehicle sounds, human bodily sounds, animal sounds) in the right superior temporal gyrus (green-blue color scale; $t \geq 2.55$, FDR $q < 0.05$; peak coordinate [57 −37 19]). An ROI analysis (Figure 1B) demonstrated increased BOLD signal for music stimuli compared to tool, animal, nature and vehicle sounds, human bodily noises, a scrambled baseline condition, and human speech. Error bars represent standard error of the mean across runs.

(legend continued on next page)

(n = 10), whose lesions were in either the left or right hemisphere, but not in the right posterior superior temporal gyrus. The neurologically intact matched controls and neurosurgery controls exhibited similar foci of increased BOLD contrast for music compared to language in the right superior temporal gyrus (green and cyan outlines, respectively, Figure 1A; see Figures S1C and S1D for whole-brain contrast maps). An analysis that quantitatively assessed the similarity of patient AE to matched healthy control participants found that he was within the range of age- and education-matched controls in terms of the location of the peak voxel in the vicinity of the right posterior superior temporal gyrus expressing "music preferences" (Figure S2).

In a second fMRI experiment, the patient passively listened to melodies and other natural and environmental sounds (e.g., animal noises, human speech, tool noises; stimuli from Norman-Haignere et al. [3]). This paradigm again identified a focus within the right superior temporal gyrus that exhibited increased BOLD contrast for music stimuli compared to the other sound categories (Figure 1B). A region-of-interest (ROI) analysis demonstrated that responses to music stimuli were greater than responses to other types of sounds (Figure 1B; see STAR Methods for details). The peak "music preferring" voxel in this experiment was shifted to the lateral surface of the superior temporal gyrus compared to the peak in the posterior Sylvian fissure observed in the first experiment. A framework within which to understand that shift may be provided by Hickok and colleagues [1], who found that rehearsal of melodies, compared to general auditory processing of melodies, led to increased BOLD contrast in the deep portion of the posterior Sylvian fissure (area Spt). Nonetheless, it is important to emphasize that the peaks for music preferences in patient AE in the two fMRI experiments were separated by less than 5 mm. The close proximity indicates good agreement across two independent approaches to localizing music preferring cortex in the posterior superior temporal gyrus in patient AE. In summary, patient AE exhibited typical neural organization for music processing that was localized to (among other regions) the right posterior superior temporal gyrus, directly adjacent to the tumor (Figure 1C).

We also assessed the patient's musical ability using the Montreal Battery of Evaluation of Amusia (MBEA), developed by Peretz and colleagues [5]. AE was correct on 177 out of 180 trials, which places him in the 89th percentile (normalized values from [5]; see Table S1). The patient's performance across each subtest of the MBEA was also within the range of a group of music-education-matched control participants (Figure 1D). Note as well that a subset of those same controls completed the fMRI protocol to map melody processing (Figure 1A, green outline; Figure S1C).

In preparation for the awake mapping procedure, patient AE practiced a modified version of the melody and sentence repetition task that had been used in fMRI and also practiced playing a piece of music on his saxophone that was modified to reduce the number and duration of long notes that would be played intraoperatively (see STAR Methods).

Intraoperative Electrical Stimulation Mapping

The awake mapping session was organized into three phases, in the following order: picture naming, intermixed sentence and melody repetition, and melody repetition. The patient did not make any errors on any trials from the language tasks (picture naming and sentence repetition), regardless of where electrical stimulation was delivered (see below). During the melody repetition trials, AE listened to and immediately repeated 74 melodies; 36 of those trials were performed in conjunction with direct electrical stimulation to the right middle or superior temporal gyri, or inferior parietal cortex. Trials were separated, offline, into correct (completely acceptable responses), minor errors (acceptable performance but minor errors in pitch, rhythm, and/or contour), and major errors (major errors in pitch, rhythm, and/or contour). The category of "major error" included what we refer to as "music arrest"—a transient inability to hum a melody (see Movie S1 for examples of errors and correct trials during intraoperative music mapping).

Patient AE made a total of 8 major errors, all of which occurred after direct electrical stimulation of the right superior temporal gyrus (see Figure 2A). On 4 additional stimulation trials, AE made minor errors in pitch, rhythm, and/or contour (see Figure 2A, cyan stimulation points; see STAR Methods for detailed discussion of error types and Movie S1 for examples). AE never made errors in rhythm or tempo in isolation; all responses marked by errors in rhythm and/or tempo also contained errors in pitch. While the exigencies of the mapping session prevented stimulation of a broad expanse of cortex, it was the case that stimulation delivered to structures other than the superior temporal gyrus, in particular the middle temporal gyrus, did not result in major errors (Figure 2C).

It is noteworthy that the patient at times spontaneously reported when his reproduction of a melody was incorrect and was generally aware that he was making errors. For instance, he noted, after stimulation events of the superior temporal gyrus, that his humming response "did not feel right" or that his experience on that trial "was weird" (e.g., see Movie S1). However, the patient was unaware on which trials his brain was being stimulated, when stimulation was being delivered on a given trial, or where in his brain the stimulation was delivered.

An important question that can be addressed with this dataset is the degree to which pre-operative fMRI relates to behavioral accuracy during direct electrical stimulation. Coordinates in MRI space were acquired in the operating room for each instance of brain stimulation during the mapping session (see STAR Methods). This permitted an analysis in which we computed the fMRI-based music-related activity for stimulation sites (i.e., voxels) associated with errors and for sites that were never associated with errors (see STAR Methods for details). We found that music-related fMRI activity was significantly stronger in voxels associated with stimulation-induced errors compared to voxels that were not associated with errors in melody repetition (Figure 2B). This finding was not dependent upon the specific contrast used to define musical preferences in the pre-operative fMRI datasets (see Figure 2B).

(C) Coronal images of music preferences overlaid on a pre-operative T2 anatomical image.
(D) Patient AE performed within control range on the Montreal Battery of Evaluation of Amusia (MBEA) pre- and post-operatively. The small decrement in AE's performance for contour discrimination post-operatively was not significantly different from controls ($t < 1$).
All error bars represent the standard error of the mean, across participants. See also Figure S1.

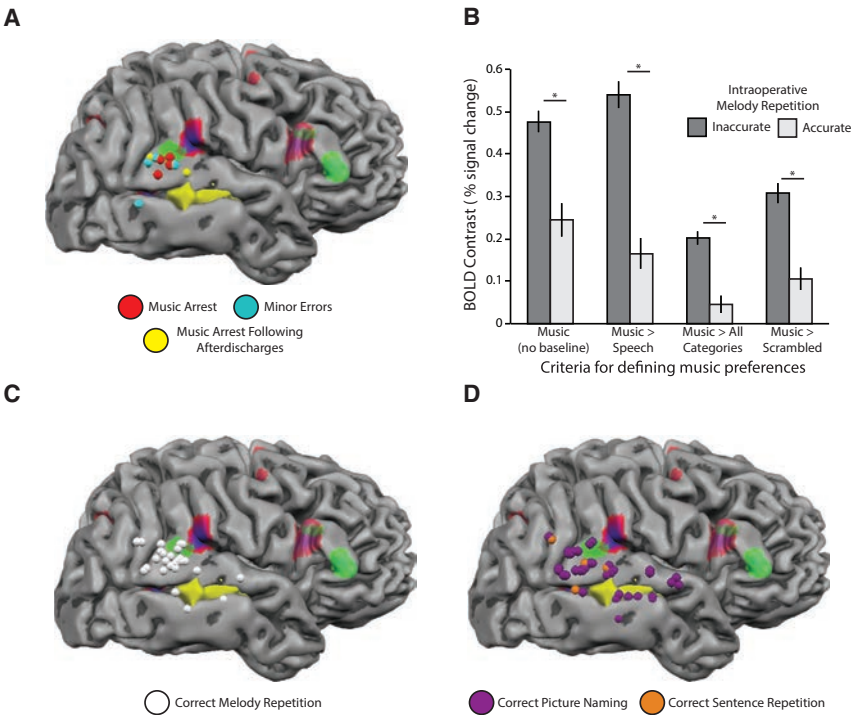

Figure 2. The Relation between Intraoperative Music Performance and Pre-operative fMRI

All intraoperative stimulation sites are represented as spheres on the cortical surface.

(A) Patient AE made 8 major and 4 minor errors in the melody repetition task after stimulation. Four of the major errors were caused by electrical stimulation on the corresponding trial (red and blue spheres); the remaining 4 major errors were caused by afterdischarges propagating from stimulation events on prior trials (yellow spheres). Two spheres are shown for trials with afterdischarges, as 1 stimulation event was associated with major errors on 3 subsequent trials, and 1 stimulation event was associated with major errors on 1 subsequent trial; 4 minor errors were associated with stimulation sites in cyan. See Movies S1 and S2 for examples of inaccurate and accurate intraoperative trials.

(B) Intraoperative melody repetition during stimulation is related to pre-operative fMRI defined music activity. fMRI voxels corresponding to stimulation sites associated with errors exhibited stronger pre-operative BOLD contrast for musical stimuli compared to functional voxels corresponding to stimulation sites that never resulted in an error; this effect was present for a range of contrasts used to define music preferences (*$p < 0.001$, unpaired samples t test). Error bars represent standard error of the mean across voxels.

(C) Stimulation sites associated with correct melody repetition are plotted in white. Stimulation of the right posterior superior temporal gyrus did not always elicit errors in melody repetition, but major errors were caused by stimulation of only that region (A).

(D) Stimulation sites associated with correct picture naming and sentence repetition trials. There was no effect of stimulation to the right posterior superior temporal gyrus on picture naming or sentence repetition trials (see also Figure S1 and Movie S2).

As shown in Figures 3 and 4, the spatial distribution of errors indicates that neither stimulation strength (Figure 3) nor the duration of electrical stimulation (Figure 4) was related to the incidence or type of errors. Specifically, major and minor errors in melody repetition were observed for the full ranges of current amplitudes (Figures 3A and 3B) and stimulation durations (Figures 4A and 4B) used throughout the mapping session. Importantly, the same values of stimulation amplitude and duration that affected melody repetition had no effect on sentence repetition or picture naming (see Figures 3D and 4D). Finally, correct melody repetition trials were associated with the full ranges of current amplitude (Figure 3C) and stimulation duration (Figure 4C) as well. These findings reinforce the conclusion that major errors in melody repetition were due to stimulation of the right superior temporal gyrus, as opposed to other parameters of the electrical stimulation.

In contrast, stimulation of the right superior temporal gyrus in AE never affected language performance (see Figure 2D for stimulation sites associated with accurate language performance). There were a total of 43 instances of direct brain stimulation during language tasks, across a combined 109 trials of picture naming and sentence repetition. Patient AE never made errors in the sentence repetition task, even after stimulation of the same region of the right posterior superior temporal gyrus that elicited errors in the similarly structured melody task (see Figure 2D; see Movie S2). A concern that may be raised is whether these intraoperative language paradigms have sensitivity to elicit language errors when critical language sites are stimulated. As a positive control, Movie S3 shows the types of language errors (phonological, speech arrest) made by patient AG, an individual undergoing language mapping of the left temporal lobe prior to a left anterior temporal lobe resection.

DISCUSSION

Much of the evidence that has elucidated the neural mechanisms of music processing comes from studies of individuals with impaired music ability (e.g., see [5–12]). MRI studies of the amusic brain have demonstrated structural abnormalities of the right inferior frontal gyrus (e.g., see [28, 29]) as well as reduced volume of the right arcuate fasciculus, a white matter tract that connects the right inferior frontal gyrus with the posterior superior temporal and inferior parietal areas [30]. Those studies suggest that amusia derives, at least in part, from abnormal connectivity between the right inferior frontal gyrus and right superior temporal gyrus [9]. While we were unable to record from the right inferior frontal gyrus in this study, it remains a possibility that electrical stimulation of the right posterior superior temporal gyrus resulted in current spread to the right inferior frontal gyrus via the right arcuate fasciculus [23]. Nevertheless, the specificity of where direct brain stimulation resulted in impaired melody repetition (but not impaired language ability) provides causal evidence about a specific role for the right posterior superior temporal gyrus, perhaps together with anatomically connected structures, in melody processing.

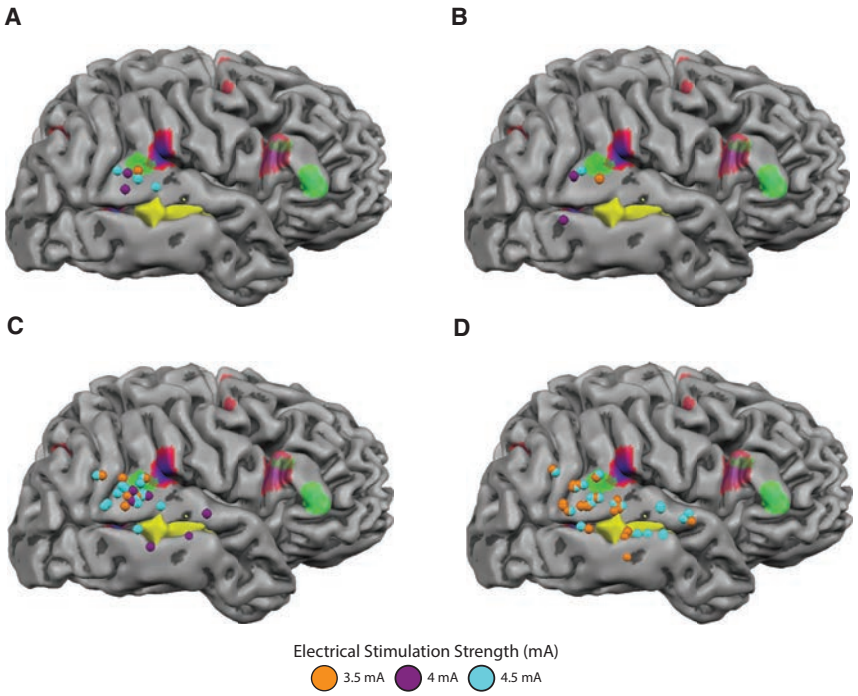

Figure 3. Modulation of Patient AE's Intraoperative Behavioral Performance as a Function of Direct Electrical Stimulation Strength

To evaluate whether the likelihood of an error was related to stimulation strength, we sought to better characterize the electrical stimulation parameters that generated major and minor errors. This analysis is possible because the surgeons vary the current amplitude throughout the mapping session to ensure that stimulation is being delivered at just below the afterdischarge threshold. Stimulation sites are recast as spheres and color coded with respect to stimulation strength (mA).

(A) Stimulation sites associated with major errors in melody repetition were associated with electrical stimulation that ranged from 3.5 to 4.5 mA, indicating that patient AE's major errors do not derive solely from stimulations with the strongest current that was delivered.

(B) Stimulation sites associated with minor errors in melody repetition were present for the full range stimulation strength that was used.

(C) Stimulation sites associated with correct melody repetition were present for the full range stimulation strength that was used.

(D) Sentence repetition and picture naming performance contained both 3.5 and 4.5 mA stimulation events.

The findings from patient AE provide causal evidence for a key component of a neurocognitive model of music processing in the brain recently advanced by Peretz [9] in which processes local to the right superior temporal gyrus are hypothesized to support pitch processing. An important goal for future research will be to understand the real-time dynamics of functional interactions between the right inferior frontal gyrus and right superior temporal gyrus when patients are repeating melodies and sentences. Future work with electrocorticography could study the dynamics that mediate interactions between the right superior temporal gyrus and right inferior frontal gyrus during melody and language processing (e.g., for evidence in the domain of language, see [31–33]; for review, see [34, 35]).

Taking a step back, there is a long history of deriving inferences about the functional organization of cognitive processes from causal data provided by detailed case studies and case series (e.g., [36–40]; for theoretical discussion, see [41, 42]). The current report is not different in that regard, as the core causal inference extracted from the results of intraoperative stimulation is that melody processing is functionally dissociable from language processing in the right superior temporal gyrus. However, issues of cortical localization of function cannot be determined on the basis of individual cases, given the known heterogeneity of local functional organization across individuals and other factors such as mass effects of a tumor. In this regard, our report is strengthened by the fact that patient AE exhibited a pattern of fMRI activity that is similar to 10 other neurosurgery patients, as well as neurologically intact age- and music-education-matched controls. Furthermore, the cortical localization of music processing to the right superior temporal gyrus that we have reported is in excellent agreement with prior studies that have identified that same brain region as being differentially engaged during music processing (e.g., [1, 2, 4]).

The clinical goal of awake mapping is to facilitate a gross-total resection of the tumor while sparing eloquent areas from damage. Evidence that this was accomplished in patient AE is provided in two forms. First, after the tumor resection was completed, but before closing of the dura, AE flawlessly played a piece of music on his saxophone (see Movie S4). Second, four weeks after his surgery, AE performed at a comparable level as he had pre-operatively on the MBEA (175/180; 85th percentile; Figure 1D; see Table S1). There was a slight drop in performance on the contour subtest of the MBEA, but that was within 1 standard deviation of control performance.

Our findings are a proof of principle that pre-operative fMRI and intraoperative mapping using a melody repetition task can be used to guide a tailored resection that preserves broader music ability in surgical interventions adjacent to cortical regions supporting music. We suggest that the melody repetition task we employed (see [1]) meets several joint constraints. First, it is a task that involves an overt and objectively quantifiable response on the part of patient, which is always preferred in an operative environment. Second, melody repetition is a task that succinctly indexes a core aspect of broader musical ability. Peretz and colleagues (e.g., see [5–12, 43]) have shown that patients with amusia are better at recognizing melodies when lyrics are present [44] and that despite poor pitch discrimination, some amusic patients can sing at levels that are comparable to control participants [26]. Those findings suggest that prior intracranial stimulation and cooling studies ([24, 25]) that employed a paradigm in which patients sing familiar songs may not index the core process that is disrupted in amusia. Future work that builds on the techniques we developed could evaluate whether focusing intracranial mapping on melody processing proves critical for preserving broader music function and avoiding a post-operative amusia.

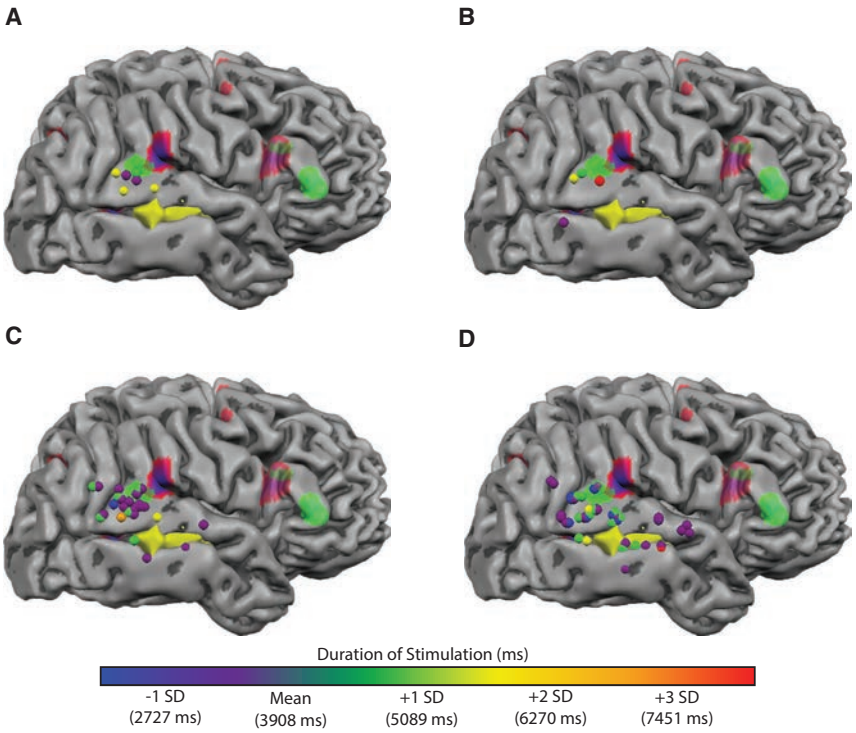

Figure 4. Modulation of Patient AE's Intraoperative Behavioral Performance as a Function of Direct Electrical Stimulation Duration

To evaluate whether error likelihood or type was related to stimulation duration, we recast stimulation sites in terms of stimulation duration. This analysis is possible because the duration of each stimulation is determined by how long the surgeon keeps the bipolar stimulator in contact with the brain. Typically, stimulation duration is 4 s, unless an error is elicited, in which case stimulation is discontinued. Stimulation events lasted between 2,235 and 7,540 ms in duration (mean = 3,908; SD = 1,109 ms).

(A) Stimulation sites associated with major errors in melody repetition were associated with electrical stimulation that ranged between 3,336 and 5,872 ms in duration (mean = 4,613 ms), indicating that patient AE's major errors do not derive from stimulations with the longest possible duration.

(B) Stimulation sites associated with minor errors in melody repetition were associated with stimulation duration that ranged from 2,869 to 7,540 ms in duration (mean = 5,130 ms).

(C) Stimulation during patient AE's correct melody repetition contained stimulations from the full range of durations.

(D) Sentence repetition and picture naming also contained stimulations from the full range of durations.

STAR★METHODS

Detailed methods are provided in the online version of this paper and include the following:

- KEY RESOURCES TABLE
- CONTACT FOR REAGENT AND RESOURCE SHARING
- EXPERIMENTAL MODEL AND SUBJECT DETAILS
  - Participants
  - Patient AE Case History
- METHOD DETAILS
  - General Experimental Methods
  - MR Acquisition Parameters
  - fMRI Stimulus Presentation Procedure
  - fMRI Experiment 1: Language and Music Repetition fMRI Experiment (Figure 1A)
  - fMRI Experiment 2: Naturalistic Sound Listening fMRI Experiment (Figure 1B)
  - fMRI Experiment 3: Object-Category Localizer (Figure S1)
  - fMRI Experiment 4: Verbal Fluency (Figure S1)
  - fMRI Experiment 5: First order motion processing (Figure S1)
  - Preprocessing of fMRI data
  - Maintaining independence of voxel definition and test
  - DTI Preprocessing and Analysis
  - Tractography of the Right Arcuate Fasciculus
  - Tractography of the Right Acoustic Radiations
  - Neuropsychological Assessment
  - Neuropsychological Assessment of Music Ability
  - Neurosurgical Intervention and Intraoperative Methods for Patient AE
  - Registration of Intraoperative Stimulation Sites to Preoperative MRI
  - Relating BOLD to Intraoperative Stimulation
  - Scoring of Intraoperative Performance
  - Intraoperative Error Types
- QUANTIFICATION AND STATISTICAL ANALYSIS
- DATA AND SOFTWARE AVAILABILTY

SUPPLEMENTAL INFORMATION

Supplemental Information includes three figures, one table, and four movies and can be found with this article online at http://dx.doi.org/10.1016/j.cub.2017.07.051.

A video abstract is available at http://dx.doi.org/10.1016/j.cub.2017.07.051#mmc7.

AUTHOR CONTRIBUTIONS

F.E.G., B.L.C., B.D., W.L., S.L.T., M.H.S., J.L., E.M., and B.Z.M. designed the study and wrote the manuscript; F.E.G., B.L.C., B.D., W.L., S.L.T., A.T., R.B., and B.Z.M. analyzed the data; S.B.G., S.E., S.O.S., J.S., L.L., T.T., B.Z.M., and W.H.P. carried out the intraoperative mapping procedure.

ACKNOWLEDGMENTS

We are grateful to all individuals who participated in these studies, in particular patients AE and AG; Gregory Hickok for sharing music stimuli [1]; Sam Norman-Haignere, Nancy Kanwisher, and Josh McDermott for sharing their sound stimuli [3]; Isabelle Peretz for making the testing materials from the MBEA available [5]; and Duje Tadin for sharing the stimuli for the first order motion fMRI experiment. We are also grateful to Keith Parkins and the URMC NeuroIT team for technical assistance in the operating room and Jeffrey Mead for assistance with the video abstract. This research was supported by NIH grant R01NSO89069 and NSF grant BCS-1349042 to B.Z.M., a core grant to the Center for Visual Science (P30 EY001319), and support to the

Department of Neurosurgery at the University of Rochester by Norman and Arlene Leenhouts. Preparation of this manuscript was supported by a University of Rochester Center for Visual Science pre-doctoral training fellowship (5T32EY007125-24) to F.E.G.

Received: April 4, 2017
Revised: June 13, 2017
Accepted: July 24, 2017
Published: August 24, 2017

REFERENCES

1. Hickok, G., Buchsbaum, B., Humphries, C., and Muftuler, T. (2003). Auditory-motor interaction revealed by fMRI: speech, music, and working memory in area Spt. J. Cogn. Neurosci. *15*, 673–682.
2. Rogalsky, C., Rong, F., Saberi, K., and Hickok, G. (2011). Functional anatomy of language and music perception: temporal and structural factors investigated using functional magnetic resonance imaging. J. Neurosci. *31*, 3843–3852.
3. Norman-Haignere, S., Kanwisher, N.G., and McDermott, J.H. (2015). Distinct Cortical Pathways for Music and Speech Revealed by Hypothesis-Free Voxel Decomposition. Neuron *88*, 1281–1296.
4. Fedorenko, E., McDermott, J.H., Norman-Haignere, S., and Kanwisher, N. (2012). Sensitivity to musical structure in the human brain. J. Neurophysiol. *108*, 3289–3300.
5. Peretz, I., Champod, A.S., and Hyde, K. (2003). Varieties of musical disorders. The Montreal Battery of Evaluation of Amusia. Ann. N Y Acad. Sci. *999*, 58–75.
6. Peretz, I., Kolinsky, R., Tramo, M., Labrecque, R., Hublet, C., Demeurisse, G., and Belleville, S. (1994). Functional dissociations following bilateral lesions of auditory cortex. Brain *117*, 1283–1301.
7. Peretz, I., Brattico, E., Järvenpää, M., and Tervaniemi, M. (2009). The amusic brain: in tune, out of key, and unaware. Brain *132*, 1277–1286.
8. Vuvan, D.T., Nunes-Silva, M., and Peretz, I. (2015). Meta-analytic evidence for the non-modularity of pitch processing in congenital amusia. Cortex *69*, 186–200.
9. Peretz, I. (2016). Neurobiology of congenital amusia. Trends Cogn. Sci. *20*, 857–867.
10. Zatorre, R.J., Belin, P., and Penhune, V.B. (2002). Structure and function of auditory cortex: music and speech. Trends Cogn. Sci. *6*, 37–46.
11. Peretz, I., Vuvan, D., Lagrois, M.-E., and Armony, J.L. (2015). Neural overlap in processing music and speech. Philos. Trans. R. Soc. Lond. B Biol. Sci. *370*, 20140090.
12. Peretz, I., and Zatorre, R.J. (2005). Brain organization for music processing. Annu. Rev. Psychol. *56*, 89–114.
13. Roux, F.E., Lubrano, V., Lotterie, J.A., Giussani, C., Pierroux, C., and Démonet, J.F. (2007). When "abegg" is read and ("A, B, E, G, G") is not: a cortical stimulation study of musical score reading. J. Neurosurg. *106*, 1017–1027.
14. Roux, F.E., Borsa, S., and Démonet, J.F. (2009). "The mute who can sing": a cortical stimulation study on singing. J. Neurosurg. *110*, 282–288.
15. Sanai, N., Mirzadeh, Z., and Berger, M.S. (2008). Functional outcome after language mapping for glioma resection. N. Engl. J. Med. *358*, 18–27.
16. Duffau, H., Gatignol, P., Mandonnet, E., Peruzzi, P., Tzourio-Mazoyer, N., and Capelle, L. (2005). New insights into the anatomo-functional connectivity of the semantic system: a study using cortico-subcortical electrostimulations. Brain *128*, 797–810.
17. Ojemann, G., Ojemann, J., Lettich, E., and Berger, M. (1989). Cortical language localization in left, dominant hemisphere. An electrical stimulation mapping investigation in 117 patients. J. Neurosurg. *71*, 316–326.
18. Roux, F.-E., Boulanouar, K., Lotterie, J.-A., Mejdoubi, M., LeSage, J.P., and Berry, I. (2003). Language functional magnetic resonance imaging in preoperative assessment of language areas: correlation with direct cortical stimulation. Neurosurgery *52*, 1335–1345, discussion 1345–1347.
19. Penfield, W., and Boldrey, E. (1937). Somatic motor and sensory representation in the cerebral cortex of man as studied by electrical stimulation. Brain *60*, 389–443.
20. Fried, I., Katz, A., McCarthy, G., Sass, K.J., Williamson, P., Spencer, S.S., and Spencer, D.D. (1991). Functional organization of human supplementary motor cortex studied by electrical stimulation. J. Neurosci. *11*, 3656–3666.
21. Desmurget, M., Reilly, K.T., Richard, N., Szathmari, A., Mottolese, C., and Sirigu, A. (2009). Movement intention after parietal cortex stimulation in humans. Science *324*, 811–813.
22. Giussani, C., Roux, F.-E., Ojemann, J., Sganzerla, E.P., Pirillo, D., and Papagno, C. (2010). Is preoperative functional magnetic resonance imaging reliable for language areas mapping in brain tumor surgery? Review of language functional magnetic resonance imaging and direct cortical stimulation correlation studies. Neurosurgery *66*, 113–120.
23. Borchers, S., Himmelbach, M., Logothetis, N., and Karnath, H.-O. (2011). Direct electrical stimulation of human cortex - the gold standard for mapping brain functions? Nat. Rev. Neurosci. *13*, 63–70.
24. Suarez, R.O., Golby, A., Whalen, S., Sato, S., Theodore, W.H., Kufta, C.V., Devinsky, O., Balish, M., and Bromfield, E.B. (2010). Contributions to singing ability by the posterior portion of the superior temporal gyrus of the non-language-dominant hemisphere: first evidence from subdural cortical stimulation, Wada testing, and fMRI. Cortex *46*, 343–353.
25. Katlowitz, K.A., Oya, H., Howard, M.A., 3rd, Greenlee, J.D.W., and Long, M.A. (2017). Paradoxical vocal changes in a trained singer by focally cooling the right superior temporal gyrus. Cortex *89*, 111–119.
26. Dalla Bella, S., Giguère, J.F., and Peretz, I. (2009). Singing in congenital amusia. J. Acoust. Soc. Am. *126*, 414–424.
27. Kay, J., Lesser, R., and Coltheart, M. (1992). PALPA: Psycholinguistic Assessments of Language Processing in Aphasia (Psychology Press).
28. Hyde, K.L., Zatorre, R.J., Griffiths, T.D., Lerch, J.P., and Peretz, I. (2006). Morphometry of the amusic brain: a two-site study. Brain *129*, 2562–2570.
29. Hyde, K.L., Lerch, J.P., Zatorre, R.J., Griffiths, T.D., Evans, A.C., and Peretz, I. (2007). Cortical thickness in congenital amusia: when less is better than more. J. Neurosci. *27*, 13028–13032.
30. Loui, P., Alsop, D., and Schlaug, G. (2009). Tone deafness: a new disconnection syndrome? J. Neurosci. *29*, 10215–10220.
31. Leonard, M.K., Cai, R., Babiak, M.C., Ren, A., and Chang, E.F. (2016). The peri-Sylvian cortical network underlying single word repetition revealed by electro cortical stimulation and direct neural recordings. Brain Lang. Published online July 19, 2016. http://dx.doi.org/10.1016/j.bandl.2016.06.001.
32. Buchsbaum, B.R., Hickok, G., and Humphries, C. (2001). Role of left posterior superior temporal gyrus in phonological processing for speech perception and production. Cogn. Sci. *25*, 663–678.
33. Chang, E.F., Niziolek, C.A., Knight, R.T., Nagarajan, S.S., and Houde, J.F. (2013). Human cortical sensorimotor network underlying feedback control of vocal pitch. Proc. Natl. Acad. Sci. USA *110*, 2653–2658.
34. Buchsbaum, B.R., Baldo, J., Okada, K., Berman, K.F., Dronkers, N., D'Esposito, M., and Hickok, G. (2011). Conduction aphasia, sensory-motor integration, and phonological short-term memory - an aggregate analysis of lesion and fMRI data. Brain Lang. *119*, 119–128.
35. Hickok, G., and Poeppel, D. (2007). The cortical organization of speech processing. Nat. Rev. Neurosci. *8*, 393–402.
36. Caramazza, A., and Hillis, A.E. (1991). Lexical organization of nouns and verbs in the brain. Nature *349*, 788–790.
37. Goodale, M.A., Milner, A.D., Jakobson, L.S., and Carey, D.P. (1991). A neurological dissociation between perceiving objects and grasping them. Nature *349*, 154–156.
38. Owen, A.M., Coleman, M.R., Boly, M., Davis, M.H., Laureys, S., and Pickard, J.D. (2006). Detecting awareness in the vegetative state. Science *313*, 1402.
39. de Gelder, B., Tamietto, M., van Boxtel, G., Goebel, R., Sahraie, A., van den Stock, J., Stienen, B.M., Weiskrantz, L., and Pegna, A. (2008). Intact

navigation skills after bilateral loss of striate cortex. Curr. Biol. *18*, R1128–R1129.

40. Finke, C., Esfahani, N.E., and Ploner, C.J. (2012). Preservation of musical memory in an amnesic professional cellist. Curr. Biol. *22*, R591–R592.
41. Caramazza, A. (1984). The logic of neuropsychological research and the problem of patient classification in aphasia. Brain Lang. *21*, 9–20.
42. Shallice, T. (1988). From Neuropsychology to Mental Structure (Cambridge University Press).
43. Peretz, I., and Hyde, K.L. (2003). What is specific to music processing? Insights from congenital amusia. Trends Cogn. Sci. *7*, 362–367.
44. Ayotte, J., Peretz, I., and Hyde, K. (2002). Congenital amusia: a group study of adults afflicted with a music-specific disorder. Brain *125*, 238–251.
45. Schwarzbach, J. (2011). A simple framework (ASF) for behavioral and neuroimaging experiments based on the psychophysics toolbox for MATLAB. Behav. Res. Methods *43*, 1194–1201.
46. Pelli, D.G. (1997). The VideoToolbox software for visual psychophysics: transforming numbers into movies. Spat. Vis. *10*, 437–442.
47. Chen, Q., Garcea, F.E., and Mahon, B.Z. (2016). The representation of object-directed action and function knowledge in the human brain. Cereb. Cortex *26*, 1609–1618.
48. Erdogan, G., Chen, Q., Garcea, F.E., Mahon, B.Z., and Jacobs, R.A. (2016). Multisensory part-based representations of objects in human lateral occipital cortex. J. Cogn. Neurosci. *28*, 869–881.
49. Garcea, F.E., and Mahon, B.Z. (2014). Parcellation of left parietal tool representations by functional connectivity. Neuropsychologia *60*, 131–143.
50. Garcea, F.E., Kristensen, S., Almeida, J., and Mahon, B.Z. (2016). Resilience to the contralateral visual field bias as a window into object representations. Cortex *81*, 14–23.
51. Chen, Q., Garcea, F.E., Almeida, J., and Mahon, B.Z. (2016). Connectivity-based constraints on category-specificity in the ventral object processing pathway. Neuropsychologia. Published online November 19, 2016. http://dx.doi.org/10.1016/j.neuropsychologia.2016.11.014.
52. Chen, Q., Garcea, F.E., Jacobs, R.A., and Mahon, B.Z. (2017). Abstract representations of object-directed action in the left inferior parietal lobule. Cereb. Cortex. Published online June 9, 2017. http://dx.doi.org/10.1093/cercor/bhx120.
53. Talairach, J., and Tournoux, P. (1988). Co-planar Stereotaxic Atlas of the Human Brain (Thieme).
54. Kriegeskorte, N., Simmons, W.K., Bellgowan, P.S., and Baker, C.I. (2009). Circular analysis in systems neuroscience: the dangers of double dipping. Nat. Neurosci. *12*, 535–540.
55. Smith, S.M. (2002). Fast robust automated brain extraction. Hum. Brain Mapp. *17*, 143–155.
56. Graham, M.S., Drobnjak, I., and Zhang, H. (2016). Realistic simulation of artefacts in diffusion MRI for validating post-processing correction techniques. Neuroimage *125*, 1079–1094.
57. Jenkinson, M., and Smith, S. (2001). A global optimisation method for robust affine registration of brain images. Med. Image Anal. *5*, 143–156.
58. Behrens, T.E., Woolrich, M.W., Jenkinson, M., Johansen-Berg, H., Nunes, R.G., Clare, S., Matthews, P.M., Brady, J.M., and Smith, S.M. (2003). Characterization and propagation of uncertainty in diffusion-weighted MR imaging. Magn. Reson. Med. *50*, 1077–1088.
59. Behrens, T.E., Berg, H.J., Jbabdi, S., Rushworth, M.F.S., and Woolrich, M.W. (2007). Probabilistic diffusion tractography with multiple fibre orientations: what can we gain? Neuroimage *34*, 144–155.
60. Garcea, F.E., Dombovy, M., and Mahon, B.Z. (2013). Preserved tool knowledge in the context of impaired action knowledge: implications for models of semantic memory. Front. Hum. Neurosci. *7*, 120.
61. Stasenko, A., Garcea, F.E., Dombovy, M., and Mahon, B.Z. (2014). When concepts lose their color: a case of object-color knowledge impairment. Cortex *58*, 217–238.
62. Forster, K.I., and Forster, J.C. (2003). DMDX: a windows display program with millisecond accuracy. Behav. Res. Methods Instrum. Comput. *35*, 116–124.
63. Barbarotto, R., Laiacona, M., Macchi, V., and Capitani, E. (2002). Picture reality decision, semantic categories and gender. A new set of pictures, with norms and an experimental study. Neuropsychologia *40*, 1637–1653.
64. Snodgrass, J.G., and Vanderwart, M. (1980). A standardized set of 260 pictures: norms for name agreement, image agreement, familiarity, and visual complexity. J. Exp. Psychol. Hum. Learn. *6*, 174–215.
65. Garcea, F.E., and Mahon, B.Z. (2012). What is in a tool concept? Dissociating manipulation knowledge from function knowledge. Mem. Cognit. *40*, 1303–1313.
66. Buxbaum, L.J., Veramontil, T., and Schwartz, M.F. (2000). Function and manipulation tool knowledge in apraxia: knowing "what for" but not "how". Neurocase *6*, 83–97.
67. Duchaine, B., and Nakayama, K. (2006). The Cambridge Face Memory Test: results for neurologically intact individuals and an investigation of its validity using inverted face stimuli and prosopagnosic participants. Neuropsychologia *44*, 576–585.

STAR★METHODS

KEY RESOURCES TABLE

REAGENT or RESOURCE	SOURCE	IDENTIFIER
Software and Algorithms		
MATLAB 2013a	MathWorks	https://www.mathworks.com
BrainVoyager QX 2.8.2	Brain Innovation	http://support.brainvoyager.com/available-tools/52-matlab-tools-bvxqtools.html
Brainlab	Brainlab	https://www.brainlab.com/en/surgery-products/overview-neurosurgery-products/cranial-navigation/

CONTACT FOR REAGENT AND RESOURCE SHARING

Further information and requests for resources or raw data should be directed to and will be fulfilled by the Lead Contact, Bradford Z. Mahon (mahon@rcbi.rochester.edu).

EXPERIMENTAL MODEL AND SUBJECT DETAILS

Participants

All participants had normal or corrected-to-normal vision, were native English speakers, and had no history of neurological disorders (for patients, other than their current clinical diagnosis—see below). All participants gave written informed consent in accordance with the University of Rochester Research Subjects Review Board.

Neurosurgical Patients

Patient AE (male, 26 years old—see case history below) participated pre- and post-operatively; 13 additional neurosurgical patients (6 female) participated while in the pre-surgical phase of treatment. Nine of the 13 neurosurgical controls had left hemisphere lesions; Patient AE and 4 other neurosurgical patients had right hemisphere lesions; the etiology of the lesions in the patient controls included glioblastoma, mesial temporal lobe sclerosis/epilepsy, and glioma. None of the neurosurgical patient controls had radiological abnormalities in the right posterior superior temporal gyrus. Ten of the 13 patient controls took part in the music and language fMRI experiment (Experiment 1); 9 of the 10 patient participants who completed the fMRI experiment, and three additional patients, completed the same battery of neuropsychological tests completed by Patient AE.

Healthy Adult Controls

Eleven individuals (3 female) from the Eastman School of Music at the University of Rochester took part in the study. Four of those individuals served as healthy controls in the fMRI study comparing language and music processing (Experiment 1), and also completed the MBEA; three individuals who did not participate in the fMRI experiment completed the MBEA; these graduate students were matched to Patient AE in age (min, 21 y, max, 29 y; M = 25.9, SD = 2.6 y) and education (all participants had completed an undergraduate or masters degree in music). Five additional participants associated with the Eastman School of Music rated pre-operative, intraoperative, and post-operative responses of patient AE that were generated during the melody repetition tasks.

Patient AE Case History

Patient AE is a right-handed man who was 26-years-old at the time of testing; he received a master's degree in music and education. He had his first seizure in June of 2015, at the age of 25. The seizure started with a feeling of intense déjà vu followed by an image of a face and music, neither of which Patient AE could identify. Patient AE also reported, at that time, an approximately year-long history of episodes while listening to familiar music where the music would suddenly 'sound different from what it should sound'. At other times, when exposed to sounds (e.g., the sound of a foot tapping) AE would perceive it as a voice speaking. These events occurred multiple times per week. On initial evaluation, AE's EEG was normal but MRI of the brain showed a 3.3 cm lesion undercutting the right superior temporal gyrus. This lesion was the only known risk factor for seizure. During his admission for inpatient long-term video and extracranial EEG monitoring in November of 2015, he had two events where non-verbal auditory stimuli sounded like a person speaking. Each of these events correlated with a right temporal seizure on scalp EEG. His inter-ictal EEG was notable for intermittent slowing and epileptiform discharges over the right temporal region. His seizures proved intractable to pharmacological interventions (valproate and zonisamide).

METHOD DETAILS

General Experimental Methods

Patient AE took part in a series of pre-operative fMRI experiments designed to localize music, language, and visual processing in his brain. During the pre-operative evaluation special attention was given to functions known to be represented adjacent to the tumor, in particular music processing. Patient AE also took part in a series of pre-operative neuropsychological tests that assessed his musical aptitude and general cognitive functioning. We recruited two groups of control participants against which to compare Patient AE's findings. Matched control group: Four Eastman School of Music graduate students completed the language and music fMRI experiment (Experiment 1), and also completed the Montreal Battery of Evaluation of Amusia (MBEA). Three additional Eastman School of Music graduate students were recruited to complete only the MBEA. A separate group of 4 graduate students and an Eastman School of Music professor (author EM) served as blinded raters of Patient AE's melody reproductions (see below).

MR Acquisition Parameters

Whole brain BOLD imaging was conducted on a 3-Tesla Siemens MAGNETOM Trio scanner with a 32-channel head coil located at the Rochester Center for Brain Imaging. High-resolution structural T1 contrast images were acquired using a magnetization-prepared rapid gradient echo (MP-RAGE) pulse sequence at the start of each participant's first scanning session (TR = 2530, TE = 3.44 ms, flip angle = 7 degrees, FOV = 256 mm, matrix = 256 × 256, 1x1x1 mm sagittal left-to-right slices). An echo-planar imaging pulse sequence was used for T2* contrast (TR = 2200 ms, TE = 30 ms, flip angle = 90 degrees, FOV = 256 × 256 mm, matrix = 64 × 64, 33 sagittal left-to-right slices, voxel size = 4x4x4 mm). The first 6 volumes of each run were discarded to allow for signal equilibration (4 volumes during image acquisition and 2 at preprocessing). DTI data were acquired using a single shot echo-planar sequence (60 diffusion directions with b = 1000 s/mm2, 10 images with b = 0 s/mm^2, TR = 8900ms, TE = 86ms, FOV = 256x256mm^2, matrix = 128x128, voxel size = 2 × 2 × 2 mm^3, 70 axial slices). A double-echo gradient echo field map sequence (echo time difference = 2.46ms, EPI dwell time = 0.75ms) was acquired with the same resolution as the DTI sequence, and was used to correct for distortion caused by B0 inhomogeneity.

fMRI Stimulus Presentation Procedure

Stimulus presentation was controlled with 'A Simple Framework' (ASF; [45]) written in MATLAB using the Psychophysics Toolbox [46], or E-Prime Professional Software 2.0 (Psychology Software Tools, Inc., Sharpsburg, PA). All fMRI participants viewed the stimuli binocularly through a mirror attached to the head coil adjusted to allow foveal viewing of a back-projected monitor (spatial resolution = 1400 × 1050 pixels; temporal resolution = 120 Hz; for prior studies using the same setup, see [47–52]).

Patient AE completed seven MRI scanning sessions in the months leading up to his neurosurgical intervention. The first session consisted of a T1 anatomical scan (6 min), an object-responsive category localizer experiment (25 min; Figure S1), resting state fMRI (12 min; data not analyzed herein), and a diffusion tensor imaging scan (15 min; see below and Figure S1B). The second session consisted of a word reading experiment (25 min; data not analyzed herein), a motion processing experiment (5 min), and a verbal fluency experiment (i.e., generate as many animal names as you can in 30 s; 15 min; Figure S1). In the third MRI session AE completed the language and music repetition experiment (45 min; Figure 1A). Patient AE returned for 3 additional scanning sessions in which he listened to and repeated only music stimuli; as these data added no new information (i.e., they showed the same pattern as the other music fMRI experiments), and there was some data loss due to technical issues, those findings are not analyzed herein. In the final scanning session AE took part in a naturalistic sound listening experiment (50 min; see Figure 1B).

fMRI Experiment 1: Language and Music Repetition fMRI Experiment (Figure 1A)

Design and Procedure

Patient AE and control participants (n = 10 neurosurgery patient controls, 4 age- and education-matched neurologically intact controls) listened to auditory stimuli and were cued to reproduce the stimulus by repeating it aloud. The stimuli consisted of three-second clips of piano melodies (for original materials, see [1]), or of spoken sentences from the PALPA subtest 12). Each trial began with a centrally presented oval, followed by a stimulus that was presented auditorily for 3 s; a jittered rehearsal period (12 to 20 s) followed the go cue. During the rehearsal period, participants were instructed to maintain the previously presented stimulus in memory until the word 'GO' was presented; upon the presentation of the 'GO' stimulus, the participant was instructed to hum or repeat the previously presented melody or sentence, respectively. Trials were interspersed with 16 s fixation periods in which a centrally presented oval was presented. Five trials of piano melodies and five trials of sentences were presented within a run, with the constraint that the two conditions were counterbalanced across runs (e.g., Subject 1, Run 1: Music-Sentence-Music-Sentence; Subject 1, Run 2: Sentence-Music-Sentence-Music). Patient AE completed 5 runs; the neurosurgical patient controls and matched healthy control participants completed either 4 or 5 runs; in the results reported we used five runs for Patient AE, and the first four runs for all control participants.

fMRI Experiment 2: Naturalistic Sound Listening fMRI Experiment (Figure 1B)

Design and Procedure

Patient AE passively listened to naturalistic sounds presented in a miniblock design. The sound stimuli were generously provided upon request by the authors of a previous fMRI investigation of the organization of music and speech in the brain [3]. There were 6 exemplars from each of the following categories: animal noises (e.g., cat meow), manipulable objects (e.g., hammering), vehicles (e.g., car accelerating), nature sounds (e.g., raining), bodily sounds (e.g., sneezing), human speech (e.g., a sentence) and music (e.g., a piano melody); we created a baseline condition by playing a subset of the sounds backward. During each miniblock, the word 'Listen' was presented centrally while six stimuli from a given category were presented auditorily. Miniblocks were interspersed with 12 s rest periods in which the word 'Fixate' was centrally presented. Each miniblock was repeated twice per run, with the constraint that a category of items did not repeat across two successive miniblocks. Patient AE completed 7 runs of the experiment (195 volumes per run).

fMRI Experiment 3: Object-Category Localizer (Figure S1)

Design and Procedure

To localize object-responsive areas in the brain, including tool-preferring regions, AE viewed scrambled and intact images of tools, animals, famous faces, and famous places (see [45] for details on stimuli and design). Twelve grayscale photographs of tools, animals, faces, and places were used; there were 8 exemplars of each (i.e., 8 different hammers; 8 different pictures of Matt Damon). This resulted in a total of 96 images per category, and 384 total images. Phase-scrambled versions of the stimuli were created to serve as a baseline condition. Participants viewed the images in a miniblock design. Within each twelve-second miniblock, 12 stimuli from the same category were presented for 1000 ms each (0 ms interstimulus interval), and twelve-second fixation periods were presented between miniblocks. Within each run, 8 miniblocks of intact images and 4 miniblocks of phase-scrambled versions of the stimuli were presented with the constraint that a category of objects did not repeat across two successive miniblock presentations. Patient AE completed 4 runs of the category localizer experiment (152 volumes per run; for precedent on this localizer, see [50]).

fMRI Experiment 4: Verbal Fluency (Figure S1)

Design and Procedure

At the start of each miniblock, AE was presented with a letter or word, which served as a cue to begin generating exemplars from a given category. The cues were letters (e.g., generate items that begin with the letter 'A'), semantic categories (e.g., generate items from the category of 'animals'), and actions (e.g., generate actions that are associated with 'grocery shopping'); each cue was presented for 4 s, followed by the word 'GO'; AE generated items from the cued category for 20 s, at which point he was presented with a 'STOP' cue. Miniblocks of stimulus presentation were interspersed by thirty-second fixation periods in which AE fixated on a centrally presented dot. Within each run, 2 miniblocks of letters, 2 miniblocks of objects, and two miniblocks of actions were presented, with the constraint that a condition did not repeat across two successive miniblocks. Patient AE completed three runs of the verbal fluency experiment (145 volumes per run).

fMRI Experiment 5: First order motion processing (Figure S1)

Design and Procedure

An array of moving dots was presented in a miniblock design. Sixteen-second miniblocks of moving dots were interspersed by sixteen-second periods in which the dots were stationary. AE completed one run of the motion processing experiment (135 volumes).

Preprocessing of fMRI data

fMRI data were analyzed with the BrainVoyager software package (Version 2.8.2) and in-house scripts drawing on the BVQX toolbox written in MATLAB (http://support.brainvoyager.com/available-tools/52-matlab-tools-bvxqtools/232-getting-started.html). Preprocessing of the functional data included, in the following order, slice scan time correction (sinc interpolation), 3D motion correction with respect to the first volume of the first functional run, and linear trend removal in the temporal domain (cutoff: 2 cycles within the run). Functional data were registered (after contrast inversion of the first volume) to high-resolution deskulled anatomy on a participant-by-participant basis in native space. For each participant, echo-planar and anatomical volumes were transformed into standardized space [53]. All functional data were smoothed at 6 mm FWHM (1.5 voxels), and interpolated to 3 mm^3 voxels. For all experiments, the general linear model was used to fit beta estimates to the experimental events of interest. Experimental events were convolved with a standard 2-gamma hemodynamic response function. The first derivatives of 3D motion correction from each run were added to all models as regressors of no interest to attract variance attributable to head movement. Unless otherwise noted, all contrast maps are thresholded with the strict whole-brain criterion of being significant at a False Discovery Rate of 0.05 (FDR $q < 0.05$).

Maintaining independence of voxel definition and test

Throughout, strict independence of criteria for voxel definition and test was applied (e.g., see [54]). There are two analyses in which this was critically important (Figures 1A and 1B). In Figure 1A the event related averages were extracted and analyzed to determine which condition led to a maximal response. In Figure 1B, we performed an ROI analysis to evaluate whether music stimuli exhibited

increased BOLD compared to other sound categories. For both analyses, n-1 runs of data were used to define music-preferring voxels, and the *nth* run was used to exact estimates of BOLD contrast (event related averages in the case of Figure 1A, measures of % signal change in the case of Figure 1B). In Experiment 1, this procedure was iterated across 5 functional runs and the results were averaged across runs to derive a mean event-related profile (see Figure 1A); in Experiment 2, this procedure was iterated across 7 functional runs and the results were averaged across runs to derive a mean percent signal change for all sound categories (see Figure 1B).

DTI Preprocessing and Analysis

DTI preprocessing was performed with the FMRIB Software Library (FSL; https://fsl.fmrib.ox.ac.uk/fsl/fslwiki/). FSL's brain extraction tool (BET) [55] was used to skull-strip AE's diffusion weighted and T1 images, as well as the fieldmap magnitude image. The B0 image was stripped from the diffusion weighted image, and the fieldmap was prepared using FSL's prepare fieldmap tool. Smoothing and regularization was performed using FSL's fugue tool (FSL; https://fsl.fmrib.ox.ac.uk/fsl/fslwiki/) and 3D Gaussian smoothing was applied (sigma = 4 mm). The magnitude image was then warped based on this smoothing, with the *y* dimension as the warp direction. Eddy current correction was performed using FSL's eddy_correct tool [56], which takes each volume of the diffusion-weighted image and registers it to the b0 image to correct for both eddy currents and motion. Next, the deformed magnitude image was registered to the B0 image using FSL's linear registration tool (FLIRT) [57]. The resulting transformation matrix was then applied to the prepared fieldmap. Lastly, the diffusion-weighted image was 'undistorted' using the registered fieldmap (FSL's fugue tool). Intensity correction was applied to this unwarping. Upon completion of preprocessing, FSL's DTIFIT tool was used to reconstruct the diffusion tensors. DTIFIT uses linear regression to fit a diffusion tensor model at each voxel of the pre-processed diffusion image.

Tractography of the Right Arcuate Fasciculus

Probabilistic tractography was performed using FSL's probtrackx2 tool, which uses Bayesian estimation of the diffusion parameters [58, 59]. Regions of interest (ROI) for tractography were functionally defined pre-operatively, using the peaks defined with the music and language repetition task (see Figure 1A), to define the right posterior superior temporal gyrus and the right inferior frontal gyrus. Ten-millimeter radius spheres were drawn around the fMRI-defined peak voxel and 5000 streamline samples were initiated from those spheres with a curvature threshold of 0.2 and a step length of 0.5mm. Using the network mode option in FSL, fiber tracking was initiated from each seed ROI separately and only the streamlines that passed through the other ROI were kept.

Tractography of the Right Acoustic Radiations

Probabilistic tractography was performed using probtrackx2 in FSL. Regions of interest were defined in MNI space following [59] and subsequently warped back into the patient's native diffusion space using FLIRT [56]. The seed was a cube on three axial slices covering the medial geniculate nucleus. A waypoint mask was placed on a single sagittal slice of the right auditory cortex (X = 56 mm). Multiple exclusion masks are used to exclude other fibers projecting from the thalamus. Following Behrens and colleagues [59], exclusion masks were placed on single slices at Z = −12, Z = 46, Y = −44, and Y = 4.

Neuropsychological Assessment

Patient AE and neurosurgery patient controls were tested in a quiet room at the Rochester Center for Brain Imaging. All neuropsychological testing took place with the same experimental stimuli and software, and sessions were audio and/or video recorded for offline analysis. Across all tasks, unless otherwise noted, Patient AE and controls were asked to quickly and accurately complete every trial. Each trial timed out at 10 s, or ended prior to that if/when a response was given. Trials that timed out at 10 s without responses were scored as incorrect. All picture stimuli were grayscale and 400 by 400 pixels (all in-house test stimuli can be found in [60]; see also [61]). For experiments requiring overt verbal responses, responses were spoken into a microphone and stimulus presentation was controlled with DMDX [62]. The responses were analyzed offline as wav files. All experiments that required keyboard presses were controlled with E-Prime Software 2.0.

Neuropsychological Assessment of Music Ability

Montreal Battery of Evaluation of Amusia (MBEA)

The MBEA is a battery of tests that evaluates several components of music processing. While the MBEA was not designed as a means to assess expert music ability, substantial normative data exist for this battery and it thus offers a robust and normed measure of music ability and meta-cognitive abilities related to music processing. Patient AE and control participants were given a brief overview of the six sections of the MBEA, and were instructed to begin marking their answers in a packet (for original materials, see [5]). Each participant was told to request clarification if needed. For the first four sections, the associated task involved marking whether two successive melodies were the same or different. Each pair of melodies was preceded by a warning signal, which was followed by a few seconds for the participant to mark an answer before the next warning signal. The fifth and sixth tests followed the same protocol for presentation of a warning signal, but used one orchestrated melody (i.e., a "tune") instead of two isolated melodies, and the participants were asked to differentiate between the type of meter associated with the tunes (Task 5), or to mark whether the melody had been presented in a previous subtest (Task 6). All test materials are freely available online (http://www.brams.umontreal.ca/site/assets/files/1395/peretzchampo_hyde-2003.pdf). Patient AE and control participants' performance is reported in Table S1. We used

control data reported in [5]; specifically, we used 120 participants' data such that the mean age of the participants was equivalent to Patient AE at the time of his testing (mean, 26.1 y; SD, 3.8 y).

In-house Neuropsychological Tests

Task 1: Object Decision. Each participant was asked to make reality judgments (real/unreal) over 40 line drawings of common objects. Real images were presented in their canonical form or manipulated such that their appearance was "not real" (e.g., a frog with a mouse's tail; for original materials see [63]).

Task 2: Number Identification. Each participant was asked to identify a centrally presented Arabic numeral. Numbers varied from one digit to three digits.

Task 3: Picture-Word Matching. Sixty-four black and white line drawings [64] were presented with a word below each picture; on each trial the participant was asked to decide if the picture and word were the same. The foils (i.e., 'no' trials) were systematically related to the pictures: Foils could be phonologically related (e.g., picture: pear, word: pencil), semantically related (e.g., picture: mouse, word: swan), or not related (e.g., picture: lemon, word: vase) to the target picture.

Task 4: Function Judgments. On each trial three tool stimuli were presented in a triangular organization; the top stimulus was the target, and participant was asked to decide which of the two bottom stimuli matched the top stimulus on the basis of its function or purpose of use (e.g., scissors and a knife are both used for cutting; see [65]; for precedent, see [66]).

Task 5: Manipulation Judgments. This task was identical in format to the Function Judgments task except that the participant was asked to match items by their manner of manipulation (e.g., scissors and pliers are manipulated similarly).

Task 6: Biological Motion Processing. Patient AE was asked to decide if a human figure comprised of dot configurations (biomotionlab.ca) was moving to the left or to the right of the center of the screen. The dot configurations were presented at systematically manipulated eccentricities from the center, varying up to 90 degrees to the left and right, respectively; direction was randomized from trial to trial.

Task 7: Word Reading. Patient AE was asked to read single words that varied in terms of grammatical category (e.g., nouns, verbs, functors), imageability (e.g., high or low imageability), sound-spelling regularity (regular and irregular words), and frequency (high or low frequency). All stimuli can be found in PALPA [27] subtests 31 – 33; see also [27], for precedent.

Task 8: Snodgrass Picture Naming. Two hundred and sixty black and white line drawings of animals, fruits, furniture, kitchen items, musical instruments, tools, vegetables, and vehicles were presented for participants to identify [64]. The stimuli were randomly ordered for each testing session.

Task 9: Nonword Reading. Participants were asked to name 24 three-, four-, five-, or six-character monosyllabic nonwords (PALPA subtest 36).

Task 10: Cambridge Face Memory Test. Participants were asked to discriminate among visually similar faces [67].

Task 11: Pantomime Discrimination. Eighteen videos of transitive actions were centrally presented while the experimenter verbally produced the name of two tools. On every trial the participant were asked to decide which tool is used in the action being pantomimed in the video.

Task 12: Action Decision. Two videos of an individual (FG) performing actions were presented on every trial, and the participant had to decide which was meaningful/real. Real actions (e.g., intransitive: saluting) were gestures that conveyed meaning, while 'unreal' actions were gestures that did not convey meaning but made similar use of the limbs.

Task 13: Sentence Repetition. An experimenter (AT) read aloud a sentence for the participant to repeat quickly and accurately (PALPA subtest 12).

Neurosurgical Intervention and Intraoperative Methods for Patient AE

Prior to the start of the surgery, Patient AE was comfortably positioned on this left side, with his head set in pins; he was able to view visual stimuli via a small monitor positioned in his line of sight and hear auditory stimuli via nearby speakers (see Movie S4). Following right temporal craniotomy and exposure of the cortical surface (right temporal lobe, inferior parietal and posterior frontal cortex), Patient AE was weaned from general anesthesia to participate in awake intraoperative mapping. Once awake, Patient AE's responses were captured by a directional microphone and recorded for offline analysis, and also projected via an amp and speaker system so that the surgical team could monitor his performance during the mapping session. Nine carbon tipped surface electrodes were arranged along the middle (three electrodes) and superior temporal gyri (3 electrodes), with three electrodes in supra-Sylvan cortex; the principal utility of the surface EEG was to monitor after-discharges during direct electrical stimulation. This was to ensure stimulation was being delivered at just below the after discharge threshold, and so that the clinical team would know if stimulation was causing after-discharges. Direct electrical stimulation was delivered with a bipolar Ojemann stimulator (Nicolet) ranging in amplitude from 3.5 to 4.5 mA (mean = 4.2 mA), and lasting between 2235 and 7540 ms (mean = 3908; SD = 1109 ms).

Registration of Intraoperative Stimulation Sites to Pre-operative MRI

The cortical location of direct electrical stimulation was acquired in real time during the awake mapping procedure by registering the bipolar stimulator to Patient AE's pre-operative T1 anatomical image, which was in turn registered to Patient AE's facial physiognomy using a cranial navigation system (Brainlab, Inc). The same procedure was carried out for Patient AG. All subsequent analyses to convert the intraoperative stimulation sites to pre-operative MRI space were performed offline. The stimulation sites were acquired in native T1 anatomical space, and projected into Talairach space using the transformation matrices derived from Talairaching the

native T1 anatomical data (using BrainVoyager software, see below). We verified the accuracy of each stimulation site using an overhead video recording (built into the operating lights) that recorded the entire neurosurgical procedure. Finally, a sphere was defined around each stimulation site (radius = 3 mm).

Relating BOLD to Intraoperative Stimulation

Locations of cortical stimulation were defined in MRI volume space as 6 mm spheres; this allowed transformation of stimulation points into functional voxel space. Each voxel that was stimulated was assigned an accuracy value: 0 if stimulation of that voxel elicited at least one error and 1 if stimulation of that voxel never elicited an error. We then extracted the fMRI data from all voxels in the two sets (correct and incorrect) and compared the strength of fMRI activity using unpaired samples t tests; this was done for several different ways of computing music preferences (Figure 2B).

Scoring of Intraoperative Performance

During the intraoperative mapping procedure Patient AE hummed auditorily-presented melodies; his productions, along with the elicited stimulus, were recorded and saved as wav files for offline analysis. De-identified audio files were then scored by five musically trained individuals (co-author E. Marvin, and 4 Eastman School of Music graduate student participants) who were blind to the focus of the research study. Care was taken that Dr. Marvin was, at the time of her scoring of the data, blinded as to trial identity (e.g., stimulation versus no stimulation). The remaining 4 expert raters were matched to Patient AE with respect to age and musical education, and were completely blinded as to the purpose of the procedure that led to those melody productions. The five raters were given a wav file for each repeated melody; each wav file contained the auditorily presented stimulus melody along with Patient AE's hummed response. We instructed the participants to rate the audio stimuli along 13 dimensions that would quantify the presence or absence of an error for each melody. Specifically, for each stimulus they were instructed to mark, with a 1 (presence) or 0 (absence), if the repeated melody was: 1) acceptable (given a non-singer in a stressful environment); 2) mostly correct (may have slight intonation problems); 3) Poor (performed with major and minor errors); if there were major errors in 4) pitch, 5) rhythm, or 6) contour; if there were minor errors 7) pitch, 8) rhythm, or 9) contour; if there were 10) hesitations after starting, 11) stops and/or restarts in the repetition, and 12) tempo changes (e.g., slowing down or speeding up); and lastly, 13) we asked them to rate how confident they were of their rating for each stimulus, on a scale from 1 to 5 (1 not very confident, 3 somewhat confident, 5 very confident).

Intraoperative Error Types

Major errors (n = 8) were defined as trials in which at least 4 of the 5 raters indicated that there were major errors in pitch, rhythm or contour. Four of the 8 major errors were a result of the electrical stimulation on the current trial (Figure 2A, red points); the remaining 4 major errors occurred as AE continued to repeat melodies while afterdischarges (subclinical epileptiform discharges induced by cortical stimulation) were propagating from stimulation to the superior temporal gyrus on a prior trial (Figure 2A, yellow points). In one stimulation event, afterdischarges affected 3 trials that followed; in a second stimulation event, afterdischarges affected 1 trial that followed. It is important to distinguish between major errors that were associated with hesitations and/or an inability to repeat the melody ('music arrest'), and major errors in which the rhythmic and contour structure of the target melody were preserved despite deviations in pitch; both types of errors occurred on trials in which the right superior temporal gyrus was stimulated. While the relatively sparse nature of the errors prevented quantitative analysis, the dominant error type was disruption in pitch processing, with less interference with rhythm and tempo (see Movie S1). Inspection of the spatial distribution of error types does not indicate a clear pattern in the types of errors that were elicited according to the subregion of the superior temporal gyrus that was stimulated (Figure 2A).

Minor errors (n = 4) were defined as trials in which 4 of the 5 raters indicated that, despite acceptable performance in a stressful environment, there were minor errors in pitch, rhythm and/or contour (see Figure 2A, cyan spheres). See Movie S1 for example errors. Inspection of the spatial distribution of error types does not indicate a clear pattern in the types of errors that were elicited according to the subregion of the superior temporal gyrus that was stimulated (Figure 2A).

Stimulation of the posterior superior temporal gyrus did not invariably lead to errors in melody repetition (see Figure 2C for stimulation sites associated with correct melody repetition). This is a general phenomenon observed in direct brain stimulation. For instance, in the domain of language mapping, stimulation of an eloquent area does not invariably lead to errors, but specific types of errors are associated with stimulation of specific regions and not nearby structures (e.g., see [17]). For example, Patient AG, an individual undergoing an awake language mapping procedure named 181 pictures, with direct electrical stimulation at 56 sites, and produced 5 instances of speech arrest and 16 instances of hesitations or phonemic paraphasias (for examples of Patient AG's errors, see Movie S3 and Figure S3).

QUANTIFICATION AND STATISTICAL ANALYSIS

All statistical analyses were performed in MATLAB 2013a (The Mathworks) or in BrainVoyager 2.8.2. Data throughout the manuscript are presented as the mean ± standard error of the mean (SEM), unless otherwise noted. All details related to the *n* for each experiment

(n = number of runs, and n = number of participants), and the particular statistical tests used, can be found in the manuscript and within the figure legends. Unless otherwise noted, in all fMRI analyses we corrected for multiple comparisons by using whole-brain False Discovery Rate (FDR) $q < 0.05$.

DATA AND SOFTWARE AVAILABILTY

All MATLAB scripts, and pre-processing scripts for analysis of the fMRI data in BrainVoyager, are available upon request by contacting the Lead Contact, Bradford Z. Mahon (mahon@rcbi.rochester.edu).

Current Biology, Volume *27*

Supplemental Information

Direct Electrical Stimulation in the Human Brain Disrupts Melody Processing

Frank E. Garcea, Benjamin L. Chernoff, Bram Diamond, Wesley Lewis, Maxwell H. Sims, Samuel B. Tomlinson, Alexander Teghipco, Raouf Belkhir, Sarah B. Gannon, Steve Erickson, Susan O. Smith, Jonathan Stone, Lynn Liu, Trenton Tollefson, John Langfitt, Elizabeth Marvin, Webster H. Pilcher, and Bradford Z. Mahon

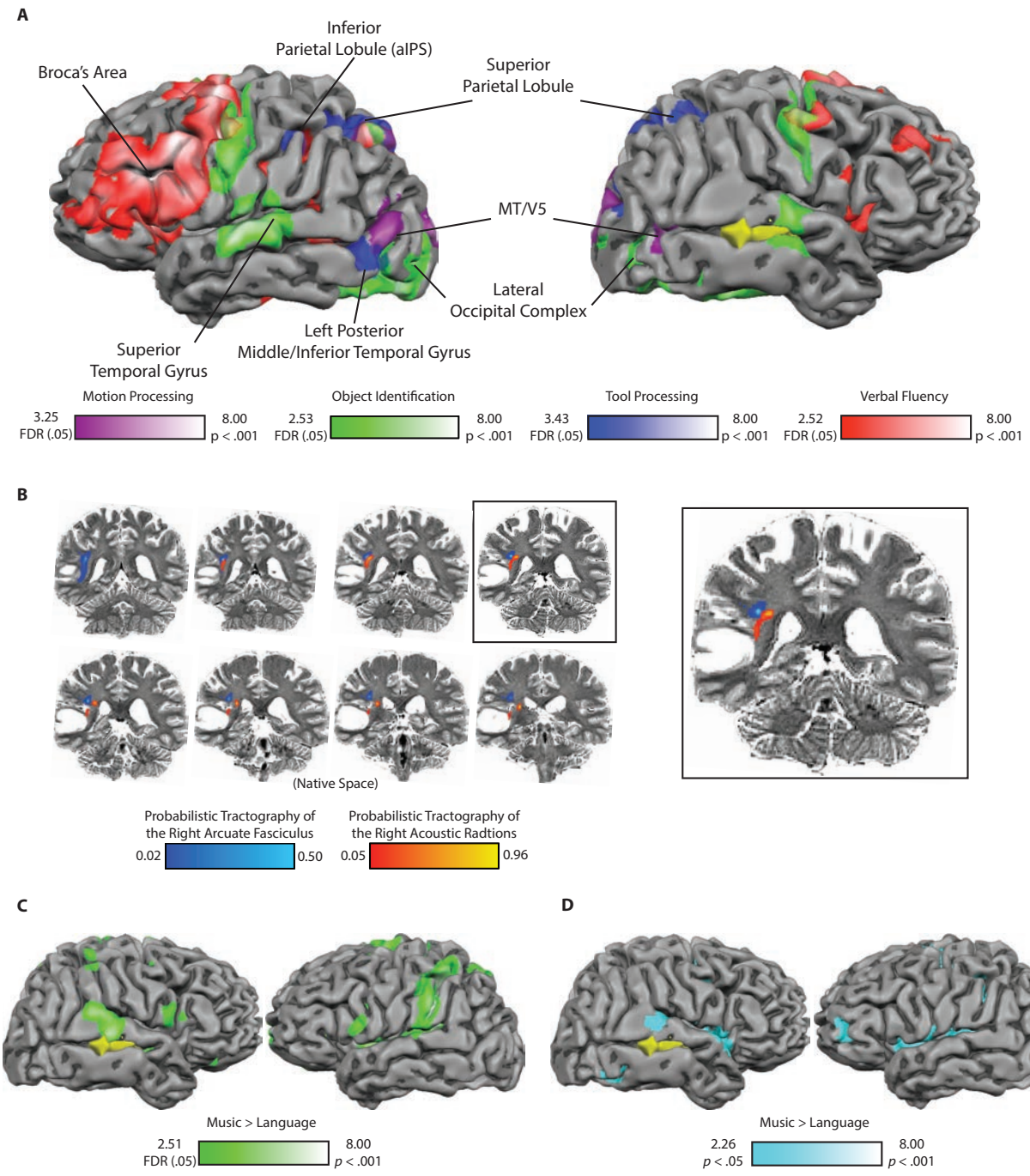
A
Broca's Area
Inferior
Parietal Lobule (aIPS)
Superior
Parietal Lobule
MT/V5
Lateral
Occipital Complex
Superior
Temporal Gyrus
Left Posterior
Middle/Inferior Temporal Gyrus
Motion Processing
3.25
FDR (.05)
8.00
p < .001
Object Identification
2.53
FDR (.05)
8.00
p < .001
Tool Processing
3.43
FDR (.05)
8.00
p < .001
Verbal Fluency
2.52
FDR (.05)
8.00
p < .001
B
(Native Space)
Probabilistic Tractography of
the Right Arcuate Fasciculus
0.02
0.50
Probabilistic Tractography of
the Right Acoustic Radtions
0.05
0.96
C
Music > Language
2.51
FDR (.05)
8.00
p < .001
D
Music > Language
2.26
p < .05
8.00
p < .001

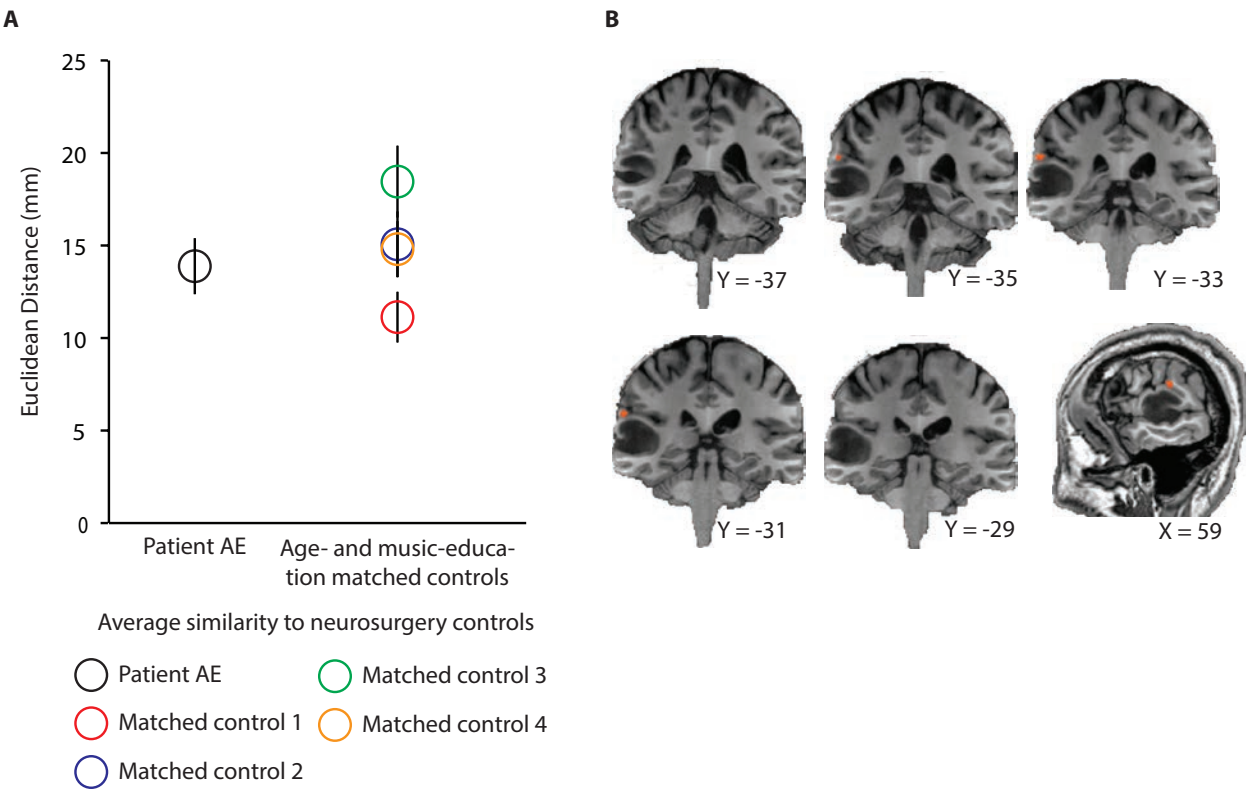
A
B
25
20
15
10
5
0
Euclidean Distance (mm)
Patient AE
Age- and music-educa-
tion matched controls
Average similarity to neurosurgery controls
Patient AE
Matched control 1
Matched control 2
Matched control 3
Matched control 4
Y = -37
Y = -35
Y = -33
Y = -31
Y = -29
X = 59

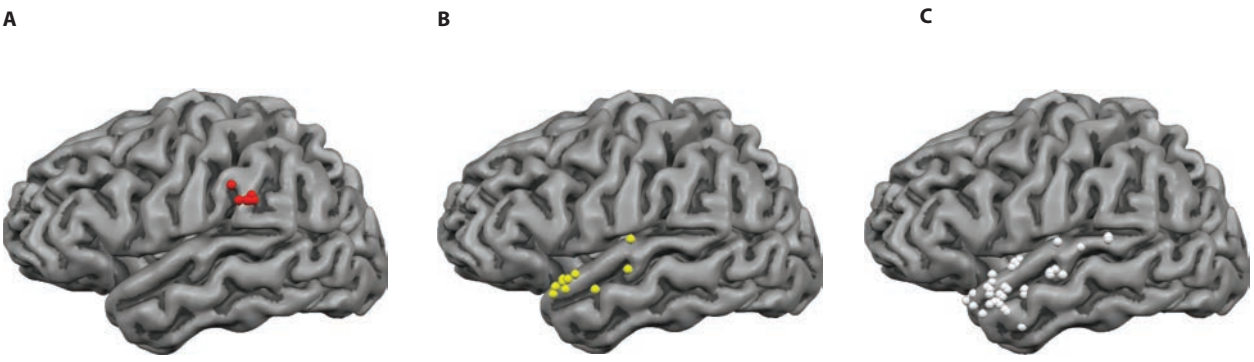
A
B
C

Figure S1. Pre-operative fMRI mapping of high-level visual processing, language production, and manipulable object processing and praxis in Patient AE's brain. A. Patient AE took part in three fMRI experiments in which we mapped high-level visual processing and language function. The tumor is represented in yellow in the right temporal lobe, visible through the expanded right superior temporal sulcus. We characterized motion-related visual activity Patient AE by asking him to attend to arrays of moving dots and contrasting BOLD contrast for moving dots against BOLD contrast for stationary dots (plotted on the purple-white color scale); this contrast identified MT/V5 bilaterally. In another experiment Patient AE fixated and named images of tools, animals, famous faces, and famous places; we contrasted those stimuli against a baseline condition in which AE fixated upon phase-shifted versions of those images (green-white color scale); that contrast identified bilateral lateral occipital complex, bilateral middle/superior temporal gyrus, and motor cortex (associated with speech motor activity). We contrasted tool stimuli against the average of animal, famous face, and famous place stimuli (equally-weighted) and identified increased BOLD contrast in the left inferior parietal lobule, bilateral superior parietal/dorsal occipital cortex, and the left posterior middle/inferior temporal gyrus (blue-white color scale; for precedent, see [*S1-S3*]). Language-related areas were identified with a verbal fluency task: BOLD contrast elicited when Patient AE produced words to letter, semantic category, and action cues compared to a resting baseline condition is shown (red-white color scale). That contrast identified the left inferior frontal gyrus (Broca's area), superior temporal/inferior parietal cortex, and the speech motor system. **B.** Pre-operative tractography showing the right acoustic radiations and arcuate fasciculus in relation to AE's tumor (5% threshold, overlaid on native T2-weighted image). **C**. Four Eastman School of Music Graduate Students took part in the music and language fMRI experiment (see Figure 1A, Experiment 1). Overlaid on Patient AE's brain in the green-white color scale (top panel) is the whole-brain contrast map of music preferences [music (perception and production) > language (perception and production)] using a fixed-effects general linear model. We observed increased BOLD contrast for music stimuli in the right superior temporal gyrus and bilaterally in temporal and parietal areas. **D**. Ten neurosurgery patients in the pre-operative phase of their treatment took part in the same experiment. Overlaid on Patient AE's brain in the cyan-white color scale (bottom panel) is the whole-brain contrast map of music preferences [music (perception and production) > language (perception and production)] using a random effects general linear model. Once again, we observe increased BOLD contrast for music stimuli in the right superior temporal gyrus. ('Figure S1. Pre-operative fMRI mapping of high-level visual processing, language production, and manipulable object processing and praxis in Patient AE's brain' related to Figure 1.)

Figure S2. Quantitative and qualitative analysis of the location of music-preferring cortex from Experiment 1. A. We defined the peak music-preferring voxel with the contrast [music perception & production] > [language perception & production] in Patient AE and in each of the control participants. One neurosurgery patient (out of 10) did not show robust music preferences in the right superior temporal gyrus with this contrast; thus, in that patient the peak voxel was defined with the contrast [music perception & production] > fixation baseline. The Talairach coordinate for the peak in Patient AE and in each control was extracted. We then computed the Euclidean distance between Patient AE and each of the 10 neurosurgery patient controls. The average distance (+/- the standard error of the mean (SEM)) is plotted in as the black circle. The same procedure was carried out for each of the age and music-education matched control participants (comparing each of those matched control participants to the 10 neurosurgery patient controls). The resulting means (+/- SEM) are plotted in the red, blue, green and orange circles. The key finding is that Patient AE is within the range established by the age- and education-matched control participants. **B.** We also qualitatively inspected the gyral anatomy in Patient AE, overlaying the peak for music preferences from Experiment 1. As can be appreciated, the peak in Patient AE is in the posterior Sylvian fissure, and likely in the posterior superior temporal gyrus just posterior to the posterior-most aspect of the Sylvian fissure (see also sagittal image). ('Figure S2. Quantitative and qualitative analysis of the location of music-preferring cortex from Experiment 1' related to Figure 1.)

Figure S3. Patient AG's intraoperative picture naming performance by error type and stimulation location. As a positive control on the sensitivity of the language mapping task to elicit errors, we report the intraoperative mapping data form Patient AG who underwent language mapping in her left temporal lobe using the same task as was used for Patient AE (see Movie S3 for examples of Patient AG's errors). **A.** Patient AG presented with speech arrest when regions in the left inferior parietal lobule were stimulated. **B.** In contrast, Patient AG presented with phonemic paraphasias when regions in the left anterior temporal lobe were stimulated. **C.** Stimulation sites associated with correct picture naming are labeled in white. Importantly, as was the case with Patient AE, stimulation of a given region did not invariably elicit an error, while there was a clear topographic distribution in the locations that when stimulated, led to an error. ('Figure S3. Patient AG's intraoperative picture naming performance by error type and stimulation location' related to Movie S3.)

Table S1. Patient AE and control participants' neuropsychological results.

	Patient AE	Patient Controls	
		Mean	SD
Object Decision	0.98	0.89	0.10
Number Identification	0.97	0.77	0.17
Picture-Word Matching	1	0.97	0.03
Function Judgments	0.92	0.96	0.07
Manipulation Judgments	0.96	0.83	0.25
Biological Motion Processing	1	0.94	0.14
Word Reading	1	0.96	0.05
Snodgrass Picture Naming	0.93	0.94	0.05
Nonword Reading	1	0.90	0.16
Cambridge Face Memory Test	0.99	0.71	0.16
Pantomime Discrimination	1	0.96	0.06
Action Decision	0.95	0.93	0.07
Sentence Repetition	1	0.93	0.14

			Control Group A (Peretz et al. [*S4*]; N = 120)		Control Group B (Seven Matched Controls)	
MBEA Subtest	Patient AE Pre-Op	Patient AE Post-Op	Mean	SD	Mean	SD
Scale	94	97	89	8.18	93	6.67
Contour	100	90	88	8.32	95	5.04
Interval	100	97	87	7.98	95	6.04
Rhythm	97	100	88	8.59	98	2.62
Metric	100	100	84	14.47	99	2.62
Memory	100	100	91	7.26	98	3.70

Table S1. Patient AE and control participants' neuropsychological results. We assessed Patient AE's broader cognitive abilities using a battery of neuropsychological tests developed and adapted in our lab, and compared his performance against a group (n = 13) of neurosurgery patient control participants in the pre-operative phase of their clinical treatment. We assessed Patient AE's musical knowledge using the Montreal Battery of Evaluation of Amusia pre- and post-operatively, and compared Patient AE's performance against two control groups. The data from Control Group A are publically available along with Peretz and colleagues' study [*S4*] (see Methods). We asked a separate cohort of age- and education-matched graduate students at the Eastman School of Music to complete the MBEA (Control Group B). Patient AE performed similarly to control participants in groups A and B when tested pre- and post-operatively. Importantly, across all neuropsychological tests, Patient AE exhibited performance that was within the normal range, typically at the upper end of the distribution or control performance. ('Table S1. Patient AE and control participants' neuropsychological results' related to STAR Methods.)

Supplemental References

S1. Chen, Q., Garcea, F. E., & Mahon, B. Z. (2016). The representation of object-directed action and function knowledge in the human brain. *Cerebral Cortex*, 26, 1609-1618.

S2. Garcea, F. E., & Mahon, B. Z. (2014). Parcellation of left parietal tool representations by functional connectivity. *Neuropsychologia*, *60*, 131-143.

S3. Garcea, F. E., Kristensen, S., Almeida, J., & Mahon, B. Z. (2016). Resilience to the contralateral visual field bias as a window into object representations. *Cortex*, *81*, 14-23.

S4. Peretz, I., Champod, A. S., & Hyde, K. (2003). Varieties of musical disorders. *Ann. New York Aca. Sci.*, *999*, 58-75.